Jestr

Journal of Engineering Science and Technology Review 14 (6) (2021) 35 - 42

JOURNAL OF
Engineering Science and Technology Review

www.jestr.org

Research Article

Accident Analysis of the Roadway Rockburst in Tangshan Coal Mine of China

Dongxu Jia[1], Jun Han[1*], Zengzhu Shi[2], Huibin Ma[1] and Chen Cao[1]

[1]*College of Mining, Liaoning Technical University, Fuxin 123000, China*
[2]*Tangshan Coal Mine, Kailuan(Group) Limited Corporation, Tangshan 063000, China*

Received 3 October 2021; Accepted 27 December 2021

Abstract

The mechanism of the roadway rockburst remains unclear, lacking necessary theoretical model. To reveal the mechanism of the roadway rockburst, taking the “8.2” rockburst accident of the Tangshan Coal Mine of China as an example, the root of the accident was examined, and a mechanical model of the roadway side coal sliding was established. The sliding instability of the roadway side coal was driven by the horizontal stress. Results show that the damage incurred by the roadway rockburst is mainly the roadway side coal sliding, accompanied with floor heave. The combination of the coal with high bearing capacity near the working face and a cantilever beam develops due to the suspended hard roof forming a “seesaw” structure. Under the high abutment pressure of the working face, the roof above the working face rebounds upwards, and the coal below loses the clamping between the roof and the floor. Eventually, the rockburst occurs as a result of the instability of the “seesaw” structure under the horizontal stress. The conclusions obtained in this study provide the theoretical foundation for roadway rockburst prevention and control, and facilitates safe and efficient production.

Keywords: Roadway, Rockburst, Slip instability, Horizontal stress

1. Introduction

Rockburst is one of the main disasters threatening the safety of underground coal mining. Due to the resource scarcity in the eastern and shallow regions of China, coal mining has gradually extended to the northwest and deep regions, and the mining intensity is increasingly higher. The rock mass structure and stress environment become more complicated, commonly leading to several geological disasters associated with dynamic impact, among which a representative and notorious one is the rockburst [1-3]. Compared with those in the shallow regions, both the intensity and frequency of the engineering disasters in the deep regions are increased [4-5].

Statistical analysis of the documented 2510 destructive rockbursts showed that rockbursts occurred in the working face, driving roadways and retrieving roadways. The rockbursts that occurred in the roadway, termed the roadway rockburst in this study, accounted for 86.8% of the total rockbursts. Among the 14 severe catastrophic rockbursts happened in 2010-2015, the proportion of the roadway rockbursts was 79%. The roadway rockburst destructed the supporting equipment, narrowed the roadway cross section, and caused casualties. The roadway cross section reduction rate was usually 50% to 70%, even up to 90%, which highly jeopardizes safe and efficient mining of the deep underground coal resources [6].

At 12:24 on August 2, 2019, Tangshan Coalmine of Kailuan (Group) Co., Ltd. experienced a severe rockburst accident, resulting in 7 deaths. This study analyzed the failure mode of the “8.2” roadway rockburst accident in Tangshan Coal Mine, examined the root of the accident, and proposed a mechanical model of the sliding instability of the roadway side coal, which is verified by in-situ coring. Therefore, it is of great significance to study the mechanism of the roadway rockburst for safety mining.

2. State of the art

The evolution and occurrence of a rockburst is extremely complex. Many researchers proposed several classic theories to explain the rockburst mechanism, including strength theory, stiffness theory, energy theory, burst-prone theory and coal clamping theory. On the basis of the above-mentioned theories, subsequent efforts including the “three criteria” theory, instability of the deformed system theory, “three factors” theory, dynamic and static load superposition theory, fractal theory, and burst initiation theory are also been proposed. The consensus on the roadway rockburst accident is that the roof and coal seam where the rockburst occurs are hard and strong.

At present, many researchers have studied the evolution and occurrence of roadway rockbursts, mainly from the aspects offundamental mechanism, energy evolution, numerical simulation, and field measurement. Qi et al. [7] proposed the mechanism of frictional sliding instability based on field observations, and suggested that the structure of coal and rock layers and the thin soft layer between are the main structural factors that cause rockbursts. Pan et al. [8] proposed the concept of critical resistance zone by theoretically analyzing the rockburst occurred in roadways, working faces, and faults, and proposed that the ratio of the slope of the pre-peak and post-peak stress-strain curve of coal is a critical parameter dominating rockbursts. According to the buckling failure of the spalled thin layer near the rock (coal) wall, Miao et al. [9] proposed a rock

*E-mail address: hanj_lntu@163.com

doi:10.25103/jestr.146.04

(coal) wall sliding crack propagation model for rockburst.. Jiang and Zhao [10] reviewed the critical factors contributing to rockburst, including geological conditions, the geological structure of the mine, and the in-situ stress environment, and made corresponding explanations by taking Henan Yima mining district as an example.

The dynamic instability of the roadway surrounding rock shall satisfy certain energy conditions, that is, energy accumulation, release and transfer [11-13]. Based on the theory of non-equilibrium thermodynamics and dissipative structure, Zhao et al. [14] obtained the meso-scale energy dissipation characteristics over evolution and occurrence of rockburst through a variety of meso-scale experiments by which the mesoscopic structure difference of coal and rock samples before and after the occurrence of a rockburst. Zhu et al. [15] established an elasto-plastic softening mechanics model for circular roadways and used the theory of elastoplastic mechanics to obtain an analytical solution of the energy in the softening zone of the surrounding rock when rockbursts occurred in circular roadways. From the perspective of the energy released by each component of the surrounding rock near the roadway, they proposed the energy criterion for roadway rockburst by examining the energy sources of roadway rockburst (coal damage energy release, energy driving of the deep coal energy, and energy driving of the roof and floor).

Theoretical explanations are commonly based on idealized simplification with many assumptions. Therefore, numerical simulations to study rockbursts have been alternatively conducted. According to the working face of different engineering geological conditions and mining technology, a numerical model can be established to simulate the stress, energy evolution of the surrounding rock of the working face under specific conditions. Wang et al. [16] simulated the stress field of the isolated working face and suggested that the energy surge of roof and floor and coal seam can be used as a precursor to judge dynamic instability. Hao et al. [17] took the Chengshan Coal Mine “7.16” rockburst accident as an example to establish a model to study the impact of three factors, including excavation time, goaf area above the coal seam, and roof strength on the elastic energy accumulation of coal and rock mass, and determined that the goaf area above the coal seam is the main controlling factor for the occurrence of this accident. Guo et al. [18] established a model of stress distribution of the roadway surrounding rock in the non-uniform stress field and the plastic zone evolution. Their numerical simulations showed that the non-uniform stress caused the butterfly-shaped plastic zone to expand in a large area during the mining process, accompanied by the release of a large amount of elastic energy; as its form evolves, the risk of rockburst increases correspondingly.

Since adequate information on the energy released by the deformation and failure of surrounding rocks over coal mining can be collected by the microseismic monitoring technique, thus it has been recently widely used to rockburst monitoring and prevention in coal mines [19, 20]. Combined with the in-situ stress and surrounding rock characteristics, some scholars revealed the evolution of the energy field in the surrounding rock according to the temporal and spatial evolution of crack propagation within the roadway surrounding rock and the following failure and instability [21-26].

In this study, taking the “8.2” rockburst accident of the Tangshan Coal Mine as the engineering background, the root of the accident was examined, and a mechanical model of the roadway side coal sliding was established. The sliding instability of the roadway side coal was driven by the horizontal stress.

The rest of this study is organized as follows. Section 3 describes the relevant background and the research methods. Section 4 gives the results and discussion, and finally, the conclusions are summarized in Section 5.

3. Accident characteristics of rockburst

3.1 Engineering background

Tangshan Coal Mine is located in Tangshan City, Hebei Province, China. It belongs to Kailuan (Group) Co., Ltd., with a mining area of 55.01 km^2 and a production capacity of 3 Mt/a. With a history of 143 years, the colliery was built in 1878 and started to produce in 1881. The main mining areas of the coalmine are currently concentrated in the Yuexu District and the South Five Districts. Coal seams No. 5, No. 8 and No. 9 are under mining, and most of the burial depth approximates to 800 m.

The geology structures of the coalfield is complex [27]. The Kailuan mining area is located on the southeast side of the Zhongchao platform (Level I structural unit)-Yanshan subsidence zone (Level II structural unit) at the southern foot of the Yanshan Mountain, and the middle section of the southern margin of the Yanshan fault folding zone on the northeastern margin of the North China Plate. The caprock structure caused by the Yanshan Cycle-Tangshan and Jixian depression folds (sags, level III structural unit) in a composite coal-bearing syncline. It includes four coal-bearing structures, namely, Kaiping syncline, Chezhoushan syncline, Jinggezhuang syncline and Xigangyao syncline. The folds are mostly asymmetrical; the northwest wing of the syncline is steep and even inverted whereas the southeast wing is comparatively gentle. Anticlines are just the opposite. The fold axis is inclined to the northwest by one side. The fault structure in the coalfield is also relatively developed. Generally, strike compressive reverse faults are developed in the steep northwestern wing, and there are also subduction compressive normal faults and oblique torsion faults. In the gentle southeast wing mainly resides normal faults of tension-tension torsion high-angled or oblique types.

As a consequence, the geological structure of Tangshan mine is also complicated. The coalmine is located at the southwest rim of the northwestern wing of the Kaiping Coalfield, and the strata trike NE-SW. Most of the main structures in the coalfield are parallel to the stratigraphic strike, and the main faults, namely, FIV, FV are sequentially lied from north to south, and their strikes are basically parallel to the stratigraphic strike (Fig. 1).

In-situ stress measurements of Tangshan Coalmine conducted in the area of the lower shaft station No. 8250 and the shaft station No. 10 showed that the stress field of Tangshan Coalmine is dominated by horizontal stress, which belongs to the geodynamic type (compression zone). The measured maximum horizontal stress varied from 29.5 MPa to 33.0 MPa, the minimum horizontal stress changed from 19.6 MPa to 21.47 MPa, and the vertical stress ranges from 20.48 MPa to 21.19 MPa. The average stress gradient of the maximum principal stress is 4.30 MPa/100 m, and the average stress gradient of vertical stress is 2.86 MPa/100 m.

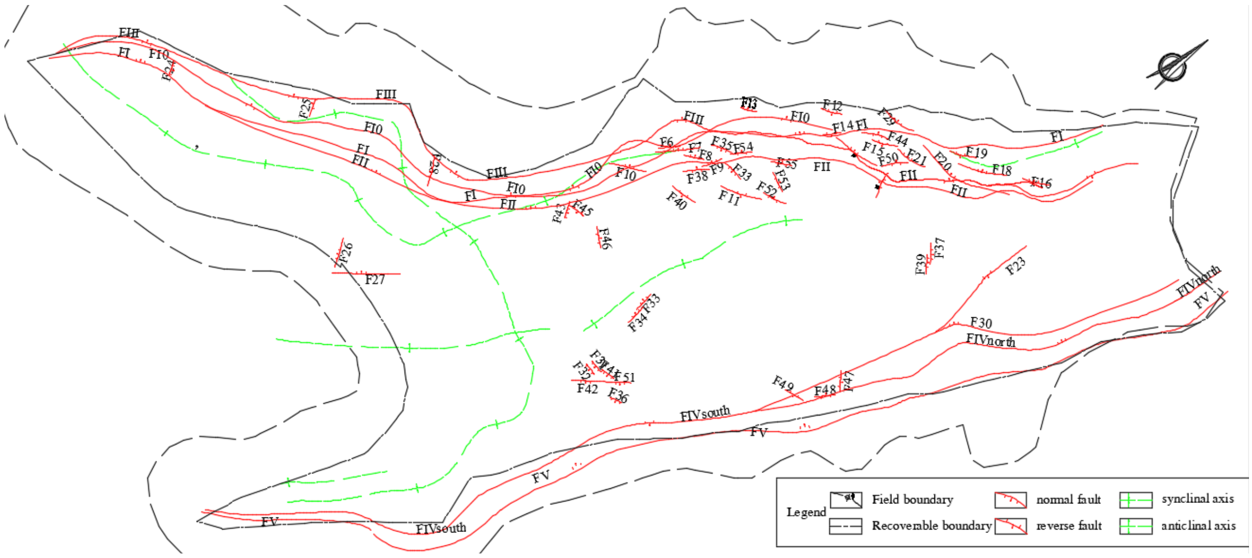

Fig. 1. Outline of the geological structure of Tangshan Coal Mine.

3.2 Description of the “8.2” rockburst accident

At 12:24 on August 2, 2019, a large rockburst accident occurred in the crossheading F5010 and the horizontal transportation pipeline F5009 in the coal pillar area of the ventilation shaft, and 7 deaths were caused. The vertical and cross-sectional views of the accident area are shown in Fig. 2. The coalmine operation center received a report from the underground that a rockburst accident occurred, and the rescue team was urgently organized to the accident location. Subsequently, other technical personnel were organized to the scene of the accident for rescue. At 20:05 of the same day, the trapped persons were discovered and lifted out of the underground, during which no further disaster occurred.

The working face F5010 is located in the coal pillar area of the ventilation shaft, the east side is belt roadway T2150, the west side is the mined-out area No. 3654, the south side are T2155, T2154, T2153, T2152 goafs, and the north side is the working face under mining F5009 and the subsidiary headgates, with ground elevation of +12.6 m to +16.6 m. The crossheading F5010 has a total length of 178 m, connecting ventilation roadway F5010, the chute F5009, ventilation roadway F5009 and the subsidiary headgate. It is tunneled along the roof of the coal seam No. 5 with an average inclination of 12°. Bolt-mesh support was adopted for support. Both the top bolt and the side bolt used the right-threaded equal-strength rebar bolt with a diameter of 20 mm and a length of 2200 mm. The top bolting spacing was 700 mm to 800 mm, and the row spacing is 800 mm. The side bolting spacing was 800 mm with a row spacing of 800 mm to 1000 m. The cable bolt was the high-strength low-relaxation pre-stressed steel wire with a diameter of 17.8 mm and a length of 6500 mm. The mesh adopted a $12^{\#}$ diamond-shaped lead wire.

After the rockburst, the crossheading F5010 was site-surveyed and Fig. 3 illustrates the roadway damage.

The accident caused the deformation of the crossheading F5010 over a length of about 80 m, of which the serious damage zone has a length of 30 m. The roadway side and floor were apparently damaged. The lower side of the roadway moved into the roadway by about 0.5 m to 2.0 m, and the upper side of the roadway was slightly damaged without obvious movement. The roadway floor was obviously damaged, and was broken near the upper side in the roadway center. The floor heave was 1.0 m to 2.5 m. From the damaged floor rock, the floor was a multi-layer composite structure.

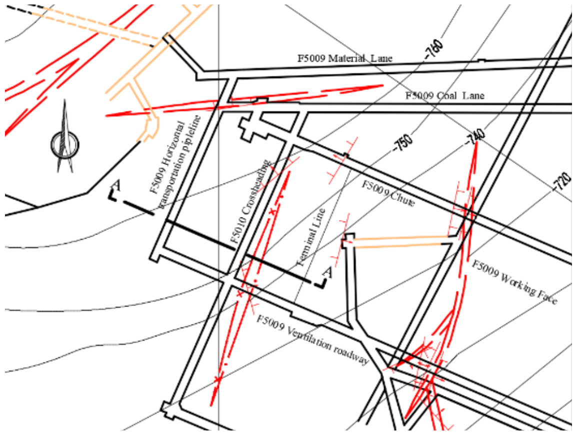

(a) Vertical view

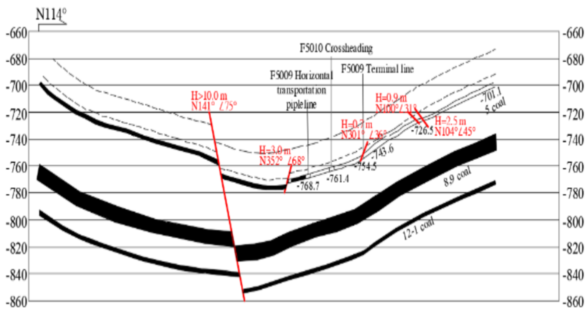

(b) Sectional view of A-A

Fig. 2. Vertical and sectional view of the region of “8.2” accident.

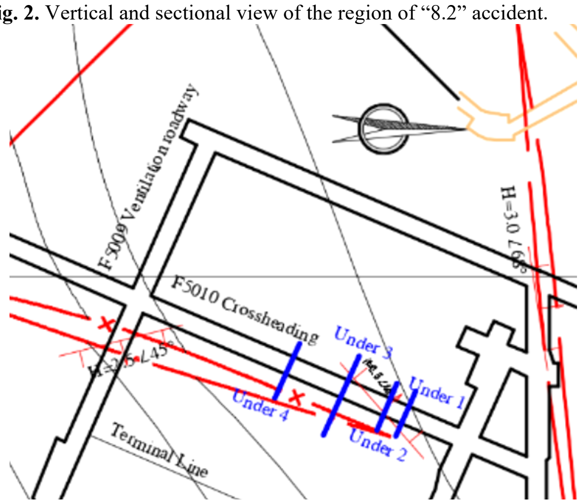

Fig. 3. Sketch of the damaged roadway location.

The details of the damage are as following:

At the location of 32.1 m upper to the lower section of crossheading F5010 (Location 1 in Fig. 4a), the height of the roadway middle was 2.6 m, the height of the upper side was 2.3 m, and the remaining height of the lower side was 0.6 m. The lower coal wall moves inside to the roadway by about 0.6 m. Floor heave occurred on the upper side (Fig. 4a).

At the location of 36.8 m up to the lower section of crossheading F5010 (Location 2 in Fig. 4a), the height of the roadway middle was 2 m, the height of the lower side was 0.5 m, the coal wall was offset to the roadway inside by about 2 m, and the height of the upper side was 1.9 m. The support steel at the roadway top was deformed to some extent (Fig. 4b).

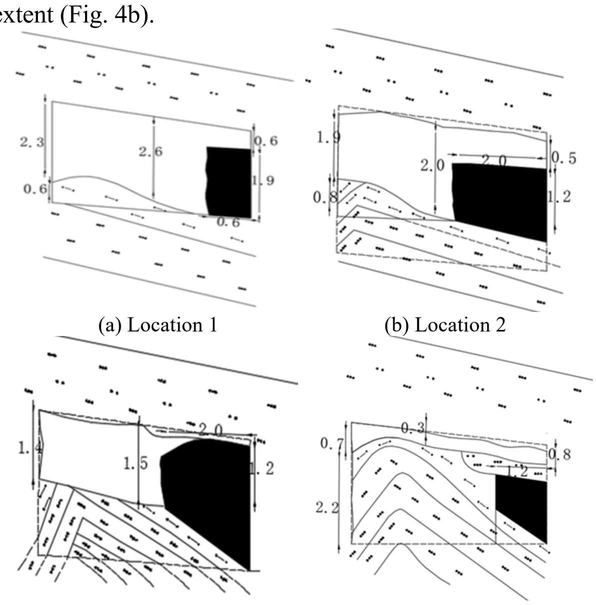

Fig. 4. Damage location of the crossheading F5010.

At the location of 47.2 m up to the lower section of crossheading F5010 (Location 3 in Fig. 4a), and the height of the roadway middle was 1.5 m. The lower coal wall was offset 2 m inside the roadway, resulting in a complete close of the roadway within 1 m of the lower side, and the upper roadway height was 1.4 m (Fig. 4c).

At the location of 61.3 m up to the lower section of crossheading F5010 (Location 4 in Fig. 4a), the height of the upper side was 0.7 m, and the minimum roadway height at a distance of 1.1 m away from the upper side was 0.3 m. The upper coal wall was offset by 1.2 m inside the roadway (Fig. 4d).

3.3 Factors contributing to the accident

Fig. 4 shows that the damage in the middle of the crossheading F5010 was the heaviest. The roadway cross-section was basically closed, and the roadway failure mode was mainly dominated by the sliding damage of the roadway side coal, accompanied by the coal rushed out from the floor damage. The accident site has complex geological structure with high tectonic stress. The measured maximum horizontal stress of Tangshan Coalmine is 29.5 MPa to 33.0 MPa, and the lateral pressure coefficient is 1.38 to 1.60, which belongs to the high in-situ stress level. Five main faults are arranged sequentially within the coalfield. The accident site is near the largest southern boundary fault FV in the coalfield.

At the same time, fold structures are developed in this area. In addition to the main direction and anticline on the south side of the FIII fault in the east, there are also a series of fold structures such as the Lingzi dip anticline on the west side, which divides the Tangshan coalfield into multiple sections. And multiple geological tectonic movements caused heavy tectonic stress concentration in this area. The accident is located at a short axial oblique axis and there is a normal fault F5009-F6 with a drop of 2.5 m nearby. The roadway axis is almost perpendicular to the maximum horizontal stress direction, which further aggravates the stress concentration degree, thus satisfying the stress condition for the rockburst.

The stress of the accident site was highly concentrated due to the influence by the mining of multiple coal seams. The industry square of the ventilation shaft where the accident site is located above a peninsula-shaped coal pillar. The coal seam No. 5, No. 8 and No. 9 in the surrounding Tie 2 District, Tie 3 District, South Wing District and East Wing District have all been mined out. The accident site was located at the border of the industry square, which was neighboring the irregular goaf of the coal seam No. 5 in the Tie 2 District. Thus, the stress distribution was complicated.

The mining-induce pressure at the accident site was high due to the superposition of the direction of the working face F5009 and the oblique abutment pressure. The crossheading F5010 was located 40 m in front of the terminal line of the working face F5009. Affected by the advanced abutment pressure of the working face, the coal pillar stress concentration in the accident site was high. The secondary stress formed by the superstition of the chute F5009 and the ventilation roadway caused the high stress concentration.

Combined with site survey of the accident, the side coal rushed into the roadway as a whole, suggesting that the horizontal tectonic stress was the force source of the accident [28-32].

4. Disaster mechanism and verification

4.1 Overlying structure Survey of the accident site

In order to ascertain the structure of the overlying strata above the coal seam No. 5 in Tangshan Coalmine, the roof sample coring approach was adopted. The roof sample coring was conducted at the horizontal transportation pipeline F5010 which is outside of the accident site. The diameter, depth, inclination angle of the drilled hole were 110 mm and 40 m, and 30°, respectively (Fig. 5).

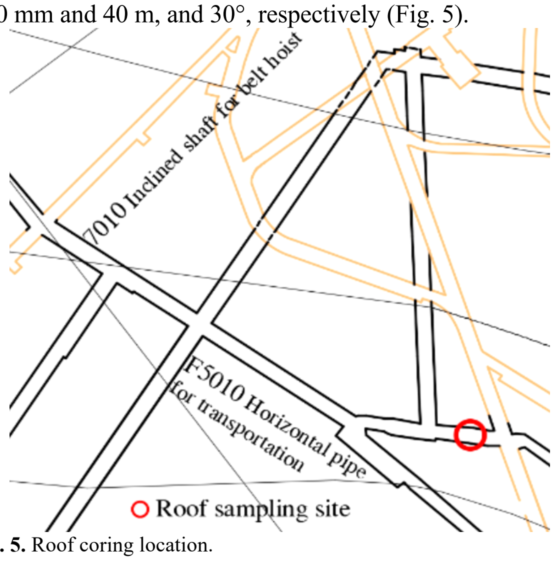

Fig. 5. Roof coring location.

A total of 41 rock cores were taken out, two of which were unlabeled and thus their lithology and depth could not be determined. According to the core labeling, three layers of roof were exposed, among which two layers were marked as siltstone and one layer was marked as medium-grained sandstone. See Table 1 for more details.

To distinguish the two layers of siltstone, according to the sampling depth, the shallow one was denoted Siltstone-1, and the deep one was termed Siltstone-2. Core labeling shows that the initial sampling depth was 2m, and the final depth was 37.5 m. Part of the cores are shown in Fig. 6.

Except that there are no cores at depth of 0 to 2 m, 8.5 m to 12.1 m, and 37.5 m to 40 m, the remaining cores are arranged according to the labelled depth, and the sampling histogram is drawn in Fig. 7. According to the histogram, the three rock layers overlying the coal seam No. 5 in the coal pillar area of the ventilation shaft of Tangshan Coal Mine are all sandstones, namely, the immediate roof is siltstone with a thickness of about 2.1 m; the basic roof is medium-grained sandstone with a thickness of about 10.9 m; and the upper part is siltstone with a thickness no less than 7 m.

Table 1. Sampled cores of roof and floor.

No.	Label No.	Depth (m)	Lithology	No.	Label No.	Depth (m)	Lithology
1	1	2~2.6	S	22	21	22~24	MGS
2	2	2.6~3.2	S	23	22	22~24	MGS
3	3	3.2~3.8	S	24	23	24~26	MGS
4	4	3.8~4.2	S	25	24	24~26	MGS
5	5	4.2~4.5	MGS	26	25	26~28	S
6	1 (6-1)	4.5~6.5	MGS	27	26	26~28	S
7	2 (6-2)	4.5~6.5	MGS	28	27	28~29.5	S
8	3 (6-3)	4.5~6.5	MGS	29	28	29.5~31.5	S
9	4 (6-4)	4.5~6.5	MGS	30	29	29.5~31.5	S
10	5 (6-5)	4.5~6.5	MGS	31	30	29.5~31.5	S
11	7	6.5~8.5	MGS	32	31	31.5~33.5	S
12	11	12.1~14.5	MGS	33	32	31.5~33.5	S
13	12	14.5~16.5	MGS	34	33	31.5~33.5	S
14	13	14.5~16.5	MGS	35	34	31.5~33.5	S
15	14	14.5~16.5	MGS	36	37	33.5~35.5	S
16	15	16.5~18.5	MGS	37	35	35.5~37.5	S
17	16	16.5~18.5	MGS	38	36-1	35.5~37.5	S
18	17	18.5~20.5	MGS	39	36-2	35.5~37.5	S
19	18	18.5~20.5	MGS	40	/	/	/
20	19	20.5~22	MGS	41	/	/	/
21	20	20.5~22	MGS				
Note	"/"denotes not labeled. MGS means the medium-grained sandstone. S means the Siltstone.						

(a) Siltstone-1 core with a sampling depth of 2 m to 4.2 m

(b) Medium-grained sandstone with a sampling depth of 4.2 m to 26

(c) Siltstone-2 core with a sampling depth of 26 m to 37.5 m

Fig. 6. Cores of three lithology.

4.2 High abutment pressure around the working face

Abutment pressure can be generated by roadway excavation and insufficient roof caving. The abutment pressure generated by the suspended roof that has not been fully caved over mining of this working face mainly acts on the coal in front of the working face. If the roof is not caved inadequately after the mining of the adjacent working face, the un-caved roof above the roadway will produce abutment pressure, which possibly affect the tailgate of the working face. After the supporting pressures of the two working faces are superimposed, the coal at the corners of the goaf side roadway in this work faces the highest vertical stress. The vertical pressure distribution around the entire working face is illustrated in Fig. 8 [33].

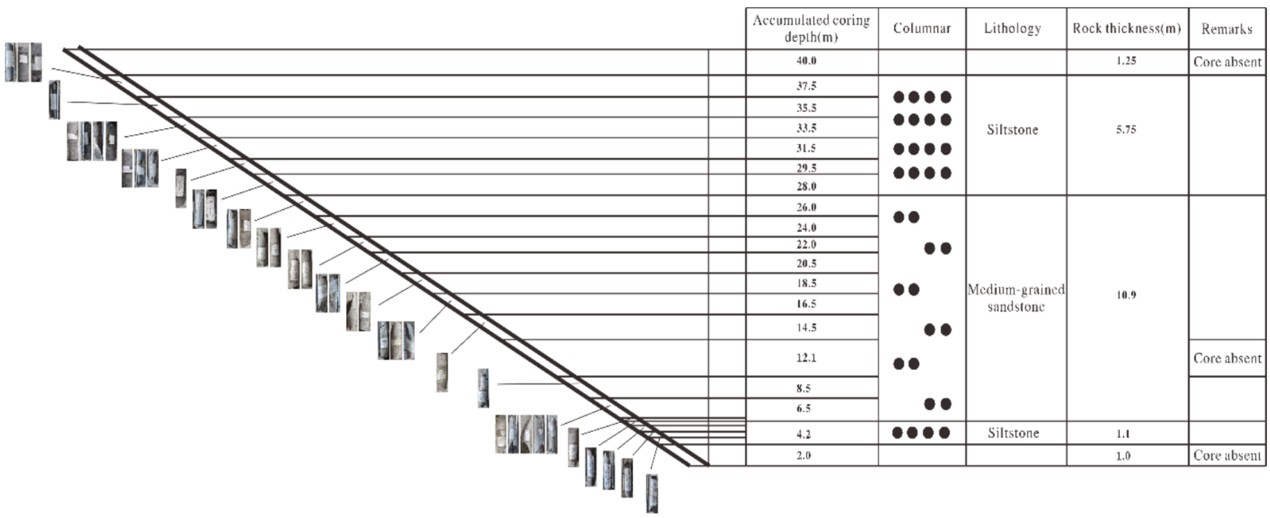

Fig. 7. Histogram of the roof under coring.

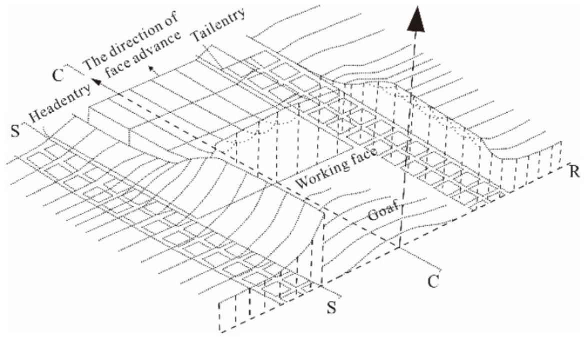

Fig. 8. Abutment pressure distribution around the working face [28].

The accident site mentioned above is located at the border of the peninsula-shaped coal pillar, surrounded by irregular working faces that have been mined, and close to the terminal line of the F5009 working face. According to the accident survey report, the roof of the coal seam No. 5 is a hard rock stratum that is not easy to cave. This likely caused a large area of the suspended roof, forming a cantilever beam structure and making the coal in front subjected to higher abutment pressure.

4.3 High coal bearing capacity

Due to the roadway excavation or the formation of other underground spaces, the original adjacent media confining coal and rock have been removed, enabling the remaining part of the stress state gradually changes from triaxial stress to bi-axial stress, or even temporarily uniaxial stress. That is the stress state of the coal/rock from the deep region of the roadway to the surface after excavation. In this stress state transition, the cracks inside the coal will be further developed and expanded due to stress concentration, leading to gradual deformation and even failure/rupture. As a result, a broken zone, a plastic zone, an elastic zone and an intact coal zone are formed from near to far away from the roadway side.

When confining pressure is present, the bearing capacity of coal can be increased significantly. Substantial true triaxial experiments have shown that the coal peak strength will increase following a power function of the confining pressure. For instance, under true triaxial conditions, a horizontal stress (σ_x) applied to the coal sample was kept at 6 MPa and the other horizontal stress (σ_y) were assigned to 0.5 MPa, 1.0 MPa and 2.0 MPa, respectively [34]. The peak compressive stress (σ_z) deforming the coal sample reached 16.6 MPa, 23.4 MPa, and 35.4 MPa, respectively. Although the confining pressure was only increased by 0.5 MPa and 1.5 MPa, respectively, the compressive strength was increased by 6.8 MPa and 18.8 MPa (Fig. 9).

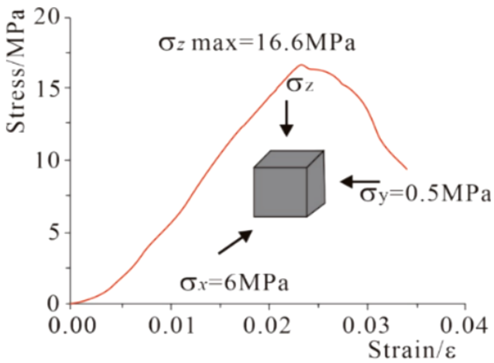

(a) 16.6 MPa

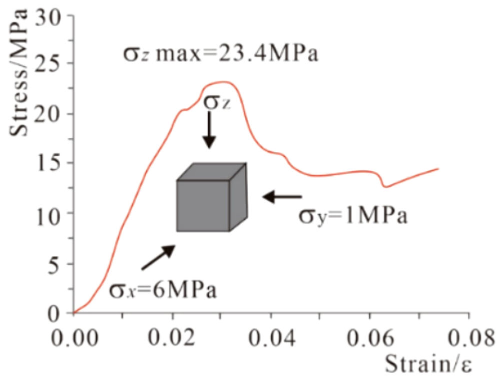

(b) 23.4 MPa

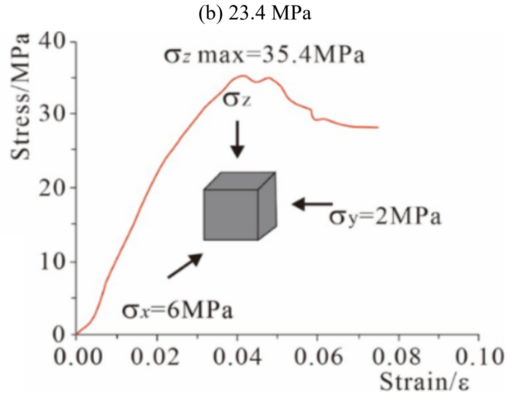

(c) 35.4 MPa

Fig. 9. Coal bearing capacity promoted with confining pressure [39].

The confining pressure of the coal in front of the working face is the horizontal, that is, the tectonic stress. At present, no reliable method has been available to accurately measure the magnitude of the tectonic stress in the coal. But crude estimation can consider it to be close to the vertical stress. Under the condition that the burial depth of the accident site of Tangshan Coalmine is around 800 m, the actual measured value of 20.48 MPa to 21.19 MPa was much higher than the confining pressure applied in Author [34]. Therefore, based on the true triaxial experiments, under high confining pressure conditions, we can safely draw the conclusion that the coal in the elastic zone and the original in-situ stress zone is still in elastic deformation state under high abutment pressure.

4.4 Roof rebound

Although the suspended roof behind the working face produces high abutment pressure, the coal near the working face owes high bearing capacity. The consequence of the interaction is that the roof above the working face rebounds upwards. The corresponding mechanism is shown in Fig. 10.

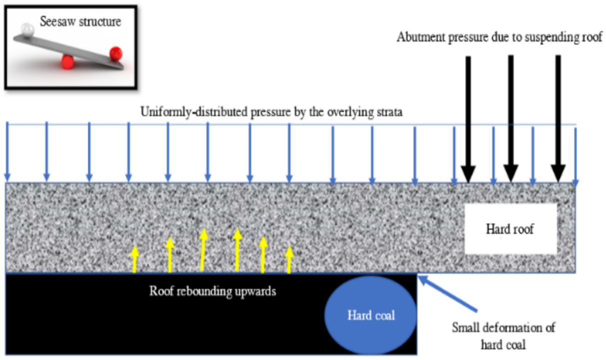

Fig. 10. Hard roof and hard coal form a seesaw structure.

The blue arrow in Fig. 10 represents the gravity of the overlying strata. The suspended roof generated by the hard roof over mining leads to a formation of a cantilever beam structure, and the generated abutment pressure is denoted by the black arrow. The coal near the working face has high load-bearing capacity, and the deformation of the coal seam in the vertical direction is small, which will inevitably cause the roof above the working face to rebound upwards, as illustrated by the yellow arrow in Fig. 10. Generally, a structure similar to a seesaw is formed in the working face. The coal near the working face is the fulcrum, and the roof near the fulcrum is the compressing plate. The abutment pressure behind the working face acting on the suspended roof causes the roof to move upward in front of the working face (Fig. 10).

4.5 Sliding and instability of roadway side coal

Assuming that both the roadway height and coal seam thickness are h, we take the coal block with a width of a along the roadway strike and the depth l at the roadway side as the study object, as shown in block A in Fig. 11. The coal block connected to block A along the roadway dip is denoted as block B, and the coal blocks connected along the roadway strike on both sides of block A are denoted as blocks C and D.

When the roof does not rebound and the model is in static equilibrium, the force equilibrium in the horizontal force is

$$\sigma_x ah = f_1 + f_2 + \sigma_T h + \mathbf{2}\tau_c hl \tag{1}$$

Where σ_x is the normal stress at the interface between blocks A and B, that is, the in-situ stress normal to the roadway side coal; σ_y is the in-situ stress along the roadway strike; N is the normal pressure acting on the roof-coal interface; f_1 and f_2 are the friction between the coal seam and the top and bottom plates, respectively; σ_T is the tensile strength between blocks A and B; τ_c is the shear strength between blocks A and C and D.

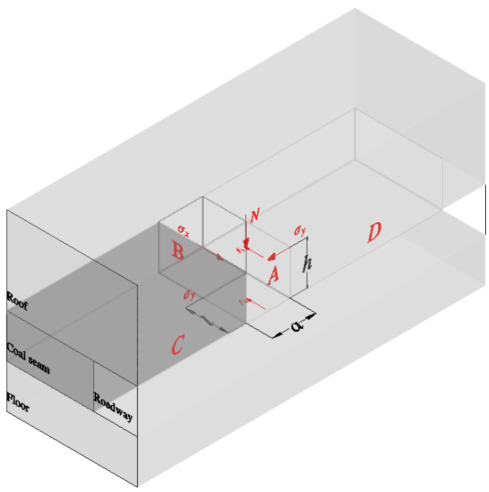

Fig. 11. Force equilibrium of the roadway side coal.

According to the Mohr-Coulomb criterion, the shear strength between block A and block C and D satisfies the following equation:

$$\tau_c = \sigma_y \tan\varphi + c \tag{2}$$

where c and φ are the cohesion and cohesive friction angle of the coal, and σ_y is the in-situ stress along the roadway strike.

Substituting Eq. (2) into Eq. (1), we get:

$$\sigma_x = \frac{f_1 + f_2}{ah} + \frac{\sigma_T}{a} + \mathbf{2}\frac{l}{a}(\sigma_y \tan\varphi + c) \tag{3}$$

As mentioned above, the axis of the roadway at the accident site is almost perpendicular to the direction of the maximum horizontal stress, that is, σ_x is the maximum horizontal stress and σ_y is the minimum horizontal stress, thus σ_x=30 MPa and σ_y=20 MPa. According to the accident site survey, the distance from the coal was 2 m, that is, l=2, and the length along the roadway strike was assumed to be 2 m, that is, a=2 m. Referring to literature [35, 36], we get the tensile strength σ_T of the coal seam No. 5 of Tangshan Coalmine is 2.4 MPa, internal friction angle φ is 20°, and cohesion c is 1.8 MPa.

When the roof rebounds, N decreases, causing f_1 and f_2 to decrease or even to zero. Substituting all the parameters into the Eq. (3), the right side of the equation is calculated to be 19.4 MPa, which is less than 30 MPa on the left side of the equation. As a consequence, coal block A becomes unstable and rushes into the roadway, causing rockburst.

5. Conclusions

Based on the “8.2” accident in Tangshan Coal Mine, this study analyzes the cause of the accident and puts forward the mechanical model of the sliding instability of the roadway side coal. The following conclusions can be obtained:

(1) The “8.2” rockburst accident was mainly caused by the sliding damage of the roadway side coal, and was accompanied by the occurrence of the floor heave. The damage in the roadway middle was more severe than those on the two sides. The largest size of the rushed-out coal was 2 m wide and 1.2 m high.

(2) Based on the failure mode of the roadway rockburst, the sliding mechanism of the roadside coal was proposed; the high abutment pressure, high coal bearing capacity and roof rebound were prerequisites. The critical criterion for the occurrence of roadway rockburst was proposed and the field data was used for the verification.

(3) Through the sample coring approach, it was determined that there was a medium sandstone with a thickness of more than 10 m in the overlying rock of the coal seam No. 5 of Tangshan Coal Mine, which verified the roof condition in the slip instability model.

This study presents a model of rock burst occurring in roadway. Parameter analysis is relatively simple at present. The next step is to carry out comprehensive parameter impact analysis and corresponding numerical simulation for this model.

Acknowledgements

This work was financially supported by the The National Natural Science Fund of China (52074145) and LiaoNing Revitalization Talents Program Grant (XLYC2002110).

References

1. Farhadian, H., "A new empirical chart for rockburst analysis in tunnelling: Tunnel rockburst classification (TRC)". *International Journal of Mining Science and Technology*, 31(4), 2021, pp. 603-610.
2. Zhao, Y. H., Wang, S. R., Zou, Z. S., Ge, L. L., Cui, F., "Instability characteristics of the cracked roof rock beam under shallow mining conditions". *International Journal of Mining Science and Technology*, 28(3), 2018, pp. 437-444.
3. Simser, B. P., "Rockburst management in Canadian hard rock mines". *Journal of Rock Mechanics and Geotechnical Engineering,* 11(5), 2019, pp. 1036-1043.
4. Tan, Y. L., Guo, W. Y., Xin, H. Q., Zhao, T. B., Yu, F. H., Liu, X. S., "Key technology of rock burst monitoring and control in deep coal mining". *Journal of China Coal Society*, 44(1), 2019, pp. 160-172.
5. Brodny, J., Tutak, M., "Analysis of methane hazard conditions in mine headings". *Technical gazette*, 25(1), 2018, pp. 271-276.
6. Lan, H., Qi, Q. X., Pan, J. F., Peng, Y. W., "Analysis on features as well as prevention and control technology of mine strata pressure bumping in China". *Coal Science and Technology*, 39(1) 2011, pp.11-15.
7. Qi, Q. X., Li, Y. Z., Zhao, S. K., Zhang, N. B., Deng, W. Y., Li, H. T., Li, H. Y., "70 years development of coal mine rockburst in China: establishment and consideration of theory and technology system". *Coal Science and Technology*, 47(9), 2019, pp.1-40.
8. Pan, Y. S., Zhang, M. T., "The exact solution for rockburst in coal mine by instability rockburst theory". *Chinese Journal of Rock Mechanics and Engineering*, S1, 1996, pp. 504-510.
9. Miao, X. X., An, L. Q., Zhai, M. H., Zhang, X. C., Yang, T. Q., "Model of rockburst for extension of slip fracture in palisades". *Journal of China University of Mining & Technology*, 28(2), 1999, pp. 15-19.
10. Jiang, Y. D., Zhao, Y. X., "State of the art: investigation on mechanism, forecast and control of coal bumps in China". *Chinese Journal of Rock Mechanics and Engineering*, 34(11), 2015, pp. 2188-2204.
11. Ching, E. S. C., Langer, J. S., Nakanishi, H., "Dynamic instabilities in fracture". *Physical review letters*, 76(7), 1996, pp. 1087-1090.
12. Yamakov, V., Saether, E., Phillips, D. R., Glaessgen, E. H., "Dynamic instability in intergranular fracture". *Physical review letters*, 95(1), 2005, pp. ID 015502.
13. Lei, J. S., Kim, B., Li, L. Y., "Dynamic instability analysis of axially compressed castellated columns". *International Journal of Steel Structures*, 20(2), 2020, pp. 559-566.
14. Zhao, Y. X., Jiang, Y. D., Tian, S. P., "Investigation on the characteristics of energy dissipation in the preparation process of coal bumps". *Journal of China Coal Society*, 35(12), 2010, pp. 1979-1983.
15. Zhu, X. J., Pan, Y. S., Li, Q., Wang, A. W., Wang, X. K., Chen, J. Q., "Softening zone energy extremum criterion and experimental study of roadway rock burst". *Journal of China University of Ming & Technology*, 50(5), 2021, pp. 975-982.
16. Wang, H. W., Jiang, Y. D., Zhao, Y. X., Liu, S., Gao, R. J., "Study on energy release mechanism of long wall isolated island working face". *Chinese Journal of Rock Mechanics and Engineering*, 32(11), 2013, pp. 2250-2257.
17. Hao, F. K., Li, H. T., Zhuo, K., Wang, H., "Study on numerical simulation of main control factors for energy distribution of mine pressure bump". *Coal Science and Technology*, 42(4), 2014, pp. 31-34.
18. Guo, X. F., Guo, L. F., Li, C., Ma, N. J., Zhao, Z. Q., Huo, T. H., "A quantitative assessment method of roadway rockburst risk based on the plastic zone shape coefficient". *Journal of China University of Mining & Technology*, 50(1) 2021, pp. 39-49.
19. Louchnikov, V. N., Eremenko, V. A., Sandy, M. P., Kosyreva, M. A., "Support design for mines exposed to rockburst hazard". *Journal of Mining Science,* 53(3), 2017, pp. 504-512.
20. Chlebowski, D., Burtan, Z., Zorychta, A., "Evaluation of rockburst hazard under abandoned mine workings". *Archives of Mining Sciences*, 63(3), 2018, pp. 687-699.
21. Wang, S. R., Li, D. J., Li, C. L., Zhang, C. G., Zhang, Y. B., "Thermal radiation characteristics of stress evolution of a circular tunnel excavation under different confining pressures". *Tunnelling and Underground Space Technology*, 78, 2018, pp. 76-83.
22. Keneti, A., Sainsbury, B. A., "Review of published rockburst events and their contributing factors". *Engineering Geology*, 246, 2018, pp. 361-373.
23. Sousa, L. R. E., Miranda, T., Sousa, R. L. E., Tinoco, J., "The use of data mining techniques in rockburst risk assessment". *Engineering*, 3(4), 2017, 552-558.
24. Manouchehrian, A., Cai, M., "Numerical modeling of rockburst near fault zones in deep tunnels". *Tunnelling and Underground Space Technology,* 80, 2018, pp. 164-180.
25. Malan, D. F., Napier, J. A. L., "Rockburst support in shallow-dipping tabular stopes at great depth". *International Journal of Rock Mechanics and Mining Sciences*, 112, 2018, pp. 302-312
26. Cheng, L., Chang, X., Wang, S. R., Wang, Y. F., Zhang, M. X., "Effect analysis of bedding plane and fracture distribution on crack propagation process in layered fractured rock mass". *Journal of Engineering Science and Technology Review*, 14(5), 2021, pp. 90-99.
27. Małkowski, P., Niedbalski, Z., Balarabe, T., "A statistical analysis of geomechanical data and its effect on rock mass numerical modeling: a case study". *International Journal of Coal Science & Technology*, 8(2), 2020, pp. 312-323.
28. Konicek, P., Schreiber, "Rockburst prevention via destress blasting of competent roof rocks in hard coal longwall mining". *Journal of the Southern African Institute of Mining and Metallurgy*, 118(3), 2018, pp. 235-242.
29. Wang, S. R., Wu, X. G., Zhao, Y. H., Hagan, P., Cao, C., "Evolution characteristics of composite pressure-arch in thin bedrock of overlying strata during shallow coal mining". *International Journal of Applied Mechanics*, 11(5), 2019, pp. ID 1950030.
30. Wojtecki, Q., Konicek, P., Schreiber, J., "Effects of torpedo blasting on rockburst prevention during deep coal seam mining in the Upper Silesian Coal Basin". *Journal of Rock Mechanics and Geotechnical Engineering,* 9(4), 2017, pp. 694-701.
31. Zhao, Y. H., Wang, S. R., Zou, Y. F., Wang, X. C., Huang, B. Q., Zhang, X. G., "Pressure-arching characteristics of fractured strata structure during shallow horizontal coal mining". *Tehnicki Vjesnik-Technical Gazette*, 25(5), 2018, pp. 1457-1466.
32. Wang, S. R., Li, N., Li, C. L., Zou, Z. S., Chang, X., "Instability mechanism analysis of pressure-arch in coal mining field under different seam dip angles". *DYNA*, 90(3), 2015, pp. 279-284.
33. Gao, Y. B., Liu, D. Q., Zhang, X. Y., He, M. C., "Analysis and optimization of entry stability in underground longwall mining". *Sustainability*, 9(11), 2017, pp. ID 2079.
34. Shen, W., Duo, L. M., He, H., Gong, S. Y., Ji, X. J., "Study on mechanism and prevention of rock burst under loading and unloading path in solid coal driving". *Journal of Mining & Safety Engineering*, 36(4), 2019, pp. 768-776.
35. Wang, F., Xu, J. L., Xie, J. L., Gou, J. K., "Pressure-relief mechanism of lower seam extraction after upper seam extraction". *Journal of Mining & Safety Engineering*, 33(3), 2016, pp. 398-402.
36. Song, P. Q., Zhu, S. J., Pan, J. N., "Tectonic stress and its influence on rock burst in Tangshan mining area". *Coal Geology & Exploration*, 40(6), 2012, pp. 34-38.